

AD-A244 322



2

# Models of the Neuronal Mechanisms of Target Localization of the Barn Owl

John Pearson, Project Director  
David Sarnoff Research Center  
Princeton, NJ 08543-5300

November 1991

Annual Technical Report - Fiscal Year 1990

Contract No.: F49620-89-C-0131

DTIC  
ELECTE  
JAN 14 1992  
S B D

Air Force  
Office of Scientific Research

DISTRIBUTION STATEMENT A  
Approved for public release;  
Distribution Unlimited

92-01099



92 1 13 013

# REPORT DOCUMENTATION PAGE

Form Approved  
GMB No. 0704-0188

Please reporting burden for this collection of information is estimated to average 1 hour per response, including the time for reviewing instructions, searching existing data sources, gathering and maintaining the data needed, and completing and reviewing the collection of information. Send comments regarding this burden estimate or any other aspect of this collection of information, including suggestions for reducing this burden, to Washington Headquarters Services, Directorate for Information Operations and Services, 1215 Jefferson Davis Highway, Suite 1204, Arlington, VA 22202-4302, and to the Office of Management and Budget, Paperwork Reduction Project (0704-0188), Washington, DC 20503.

1. AGENCY USE ONLY (Leave blank)		2. REPORT DATE November 1991	3. REPORT TYPE AND DATES COVERED Annual Tech. Report - FY 90 10 Sep 91	
4. TITLE AND SUBTITLE Models of the Neuronal Mechanisms of Target Localization of the Barn Owl			5. FUNDING NUMBERS C-F49620-89-C-0131 PE-61102F PR-3313 TA-CS	
6. AUTHOR(S) John Pearson			8. PERFORMING ORGANIZATION REPORT NUMBER	
7. PERFORMING ORGANIZATION NAME(S) AND ADDRESS(ES) David Sarnoff Research Center 201 Washington Road Princeton, NJ 08543-5300			10. SPONSORING / MONITORING AGENCY REPORT NUMBER F49620-89-C-0131	
9. SPONSORING / MONITORING AGENCY NAME(S) AND ADDRESS(ES) Air Force Office of Scientific Research			11. SUPPLEMENTARY NOTES	
12a. DISTRIBUTION / AVAILABILITY STATEMENT Approved for public release; distribution unlimited.			12b. DISTRIBUTION CODE	
13. ABSTRACT (Maximum 200 words) The major concern of this year's research was modeling the neural systems of the barn owl that perform timing comparisons of sound at the two ears with microsecond accuracy. Models of neurons in the nucleus laminaris (NL) were developed. Analysis and computer simulations were performed that demonstrated that models of these neurons that incorporate simple neuronal biophysics cannot reproduce the observed behavior of laminaris neurons. A model incorporating an abstract resonance mechanism could reproduce the experimental phenomena. These results were presented at two scientific conferences. Papers will be published from one of these conferences. Work on this project involves collaboration with the Princeton University subcontractor, who has also approached this problem from another point of view. He has developed a model neuron incorporating active channels that can reproduce the observed behavior. More analysis of the behavior of the channels will clarify their signal processing properties. Several experimental results relevant to last year's research have also been reported by scientists in the Konishi laboratory at CalTech. Changes are needed in some of the models developed last year to incorporate these results (OVER)				
14. SUBJECT TERMS			15. NUMBER OF PAGES 7	
			16. PRICE CODE	
17. SECURITY CLASSIFICATION OF REPORT Unclassified	18. SECURITY CLASSIFICATION OF THIS PAGE Unclassified	19. SECURITY CLASSIFICATION OF ABSTRACT Unclassified	20. LIMITATION OF ABSTRACT (u)	

and to investiate their functional significance.



Accession For	
NTIS GRA&I	<input checked="" type="checkbox"/>
DTIC TAB	<input type="checkbox"/>
Unannounced	<input type="checkbox"/>
Justification	
By	
Distribution/	
Availability Codes	
Dist	Avail and/or Special
A-1	

# I. BACKGROUND

The barn owl can hunt in total darkness, recognizing and locating prey by hearing alone. One component of this behavior is a very accurate head-orienting response to salient sounds (the head must rotate as the eyes are immobile). This head saccade centers the sound-producing object for closer visual and acoustic scrutiny, prior to aerial attack. Study of this system promises to reveal general principles of the nervous system's approach to three types of problems: sensory encoding and processing, multi-sensory integration, and sensorimotor interaction. Considerable progress has been made in the last 18 years in determining the acoustic and neural bases of the head saccade.

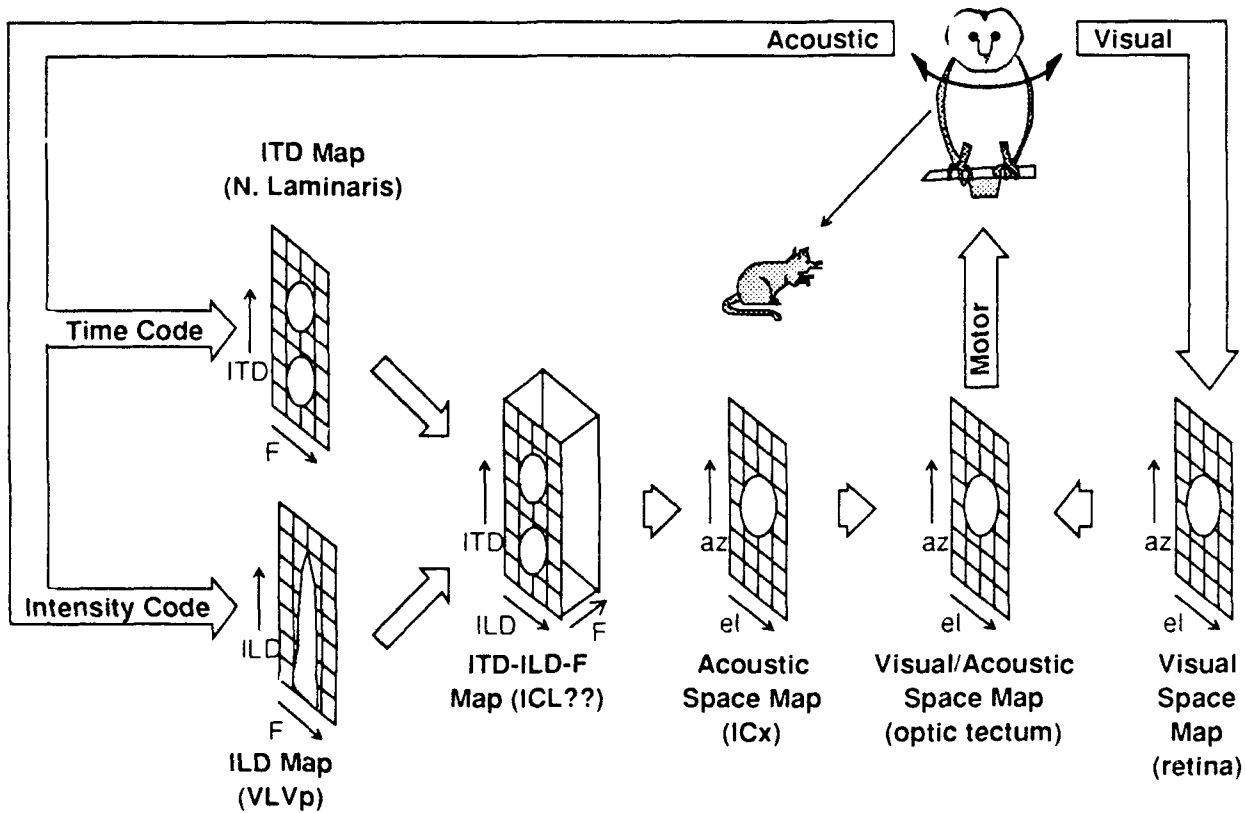


**Fig. 1** Overview of the neural system for auditory localization of the barn owl. The grids indicate the map-like representation of information at each processing stage. Acronyms such as VLVp, ICL, and ICx are defined in the text. Arrows indicate the direction of signal flow.

It is known that (see Fig. 1, above): the azimuth and elevation of the sound source direction are encoded at the periphery by, respectively, the inter-aural time difference (ITD) and the inter-aural level difference (ILD); sound intensity and timing information is processed by two parallel

streams before being recombined in a map-like representation of sound direction in the inferior colliculus (ICx); the optic tectum contains a fused visual/auditory/motor representation of stimulus and head saccade direction. The visual/auditory sensory fusion is dynamically recalibrated while the head is growing, with the auditory map in the tectum adapting to realign with the tectal visual map.

## **II. OBJECTIVES**

The purpose of this project is to further the understanding of this system through the development of biophysical and computational models and computer simulations. This work will produce explicit, testable predictions for neuroscience. In addition, it is expected that this research will lead to new artificial neural network designs, with applications for signal processing, sensory fusion, and sensorimotor integration. The following is the Statement of Work (for Year 2) contained in the project proposal:

- Task 1** Develop alternative model of sensory fusion in which the acoustic plasticity occurs in the ICx and earlier, based on the model of basic ICx function developed in Year 1 (Item #3, from Year 1).
- Task 2** Extend laminaris model developed in Year 1 (Item #2) to the bio-physical level to explain signal processing properties in low-level neuronal terms.
- Task 3** Continue development of head saccade motor system models (see Appendix C of proposal) in order to explain how sensory information of acoustic target position is translated into motor signals for head orientation towards target position.

## **III. STATUS**

### **A. Task 1**

This task was not performed this year. The model of basic ICx function needed to carry out this task is not yet complete, as we are awaiting experimental verification of it.

## B. Task 2

Neurons in nucleus laminaris receive input from both nuclei magnocellularis. Magnocellularis neurons generate action potentials that are phase-locked to the stimulus (up to 10 kHz) and nearly independent of intensity. Laminaris neurons are tuned to a particular frequency band and inter-aural phase difference or time delay. This timing system is remarkably precise, with individual neurons being sensitive to time delays as small as 10  $\mu$ s. Magnocellularis axons course

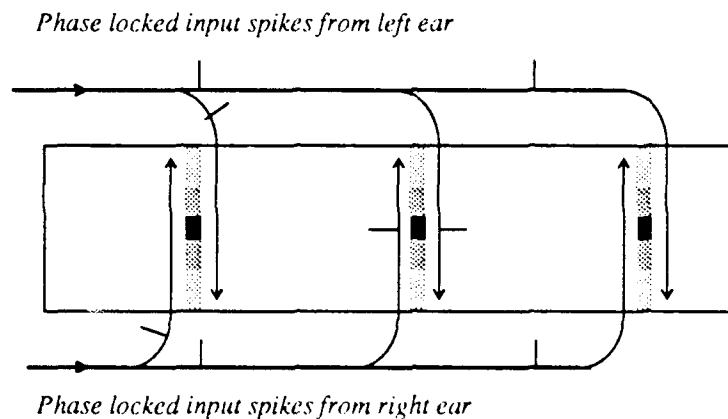


**Fig. 2** Schematic diagram of an isofrequency slab of N L. The tick marks on the axons represent action potential pulses in the axons. The shaded bars in NL between the parallel axons represent the degree of excitation of NL neurons, with darker shading representing greater excitation. NL neurons are best stimulated by coincident bilateral input from NM.

through laminaris in a manner suggestive of a coincident delay line mechanism (see Fig. 2. above), and this in fact has been the dominant type of model in the literature. However, these models have been specified at rather high levels of abstraction, in which individual neurons are assumed capable of detecting coincidences in the arrival of action potentials with a resolution of 10  $\mu$ s. This and a variety of other reasons suggested to us that such models are untenable.

To further illustrate this, we developed an approximate approach to the computation of a simple neuron model's signal processing properties, including its response to realistic input from magnocellularis. To verify the conclusions of that approach we also simulated the behavior of the model neuron. The conclusion of that work is that a neuron with a single passive compartment cannot reproduce a laminaris neuron's response to stimuli, no matter how fast the neuron's time

constants are. The reason for this is that the stimulus is encoded as a spike train (or a large number of spike trains). The spikes are only statistically phase-locked, and have considerable jitter about the optimal phase. Also the number of spikes arriving during one period of the stimulus can have large fluctuations. These effects represent noise. A standard passive neuron acts as a low-pass filter, which can only suppress noise above some frequency. The remaining low frequency noise is larger than the signal for a fairly realistic spike train from magnocellularis neurons.

Last year we studied such a mechanism by modeling a neuron as a damped harmonic oscillator that is kicked by each incoming action potential. Magnocellularis spike trains were modeled by Poisson processes whose rates are modulated by the sound's instantaneous pressure, or as Poisson processes at some constant rate if there is no sound. This work ignored the signal processing properties of the synaptic mechanism and cell membrane electrical properties. To take these into account we repeated the computations and simulations described in the preceding paragraph on a model similar to the single compartment model described above, but with the membrane potential driving a damped harmonic oscillator. There is a potential conflict between the response latency of such a neuron and its ability to respond to high frequency stimuli. The response latency is roughly given by the oscillator's damping time, but the longer the damping time, the better the oscillator will be at amplifying the signal and rejecting the noise. We chose to set the damping time to 1 msec. Recently, we have heard of indirect evidence that laminaris' latency may be as long as 20 msec (H. Wagner, private communication). This can discriminate between in-phase and out-of-phase stimuli, given reasonable values for the membrane and synaptic time constants. A paper [1] describing this work in detail can be found in Appendix A.

The oscillator model is abstract, in the sense that we are not proposing a biophysical mechanism. The model also uses an effective mechanism that would seem to require fairly exotic biophysics. There are several ordinary possibilities for improving a model neuron's ability to mimic a real laminaris neuron. One of these is the extended structure of a neuron, which could be simulated by a multiple compartment model. However, it is hard to see how this could improve the neuron's response to a particular high frequency, since such a network of compartments would act as

a network of low-pass filters. Another possibility is that active channels may have peculiar behavior. An effective model of the behavior of active channels is Hill's model, which simply employs an adaptive threshold. The threshold adapts to slow variations in the membrane potential, and so could effectively filter out low-frequency noise. A more detailed model might employ the Hodgkin-Huxley equations to accomplish the same thing. Dr. Sullivan has simulated such a model, which gave good results. A manuscript [2] describing his work is in Appendix B.

### **C. Task 3**

This task was not performed this year. Task 3 will be performed as time and interest dictate.

### **D. Other Related Work**

Some of our work this year has been a continuation of Task 3 from last year, in particular the development of models for the ILD maps in VLVp and ICL (see Fig. 1) [3, 4, 5, 6]. An alternative to our criss-cross model of the interconnection of the two VLVps was suggested by Ralph Adolphs. In principle, the alternative requires more careful adjustment of the system by the owl, but that does not make it obviously wrong. Experimental work is needed to decide which is correct, if either is, but this may be difficult. Also, our model of elevation processing in the ICL assumed that VLVp projected to the contralateral ICL and not the ipsilateral ICL. Bilateral projection has since been observed (R. Adolphs, private communication). Some of the previous simulations need to be repeated using a model that incorporates these findings.

In addition to his role as consultant to the research effort at Sarnoff, Dr. Sullivan has pursued a number of neurocomputational research topics related to the theme of this contract. Several manuscripts are in preparation (see Section IV, on page 6), and a draft version of one manuscript is included in Appendix C.

## **IV. PUBLICATIONS**

[1] Pearson, J.C., Spence, C.D. and Adolphs, R., "Model of the origin of neuronal selectivity for binaural intensity difference in the barn owl." Proceedings of the second Analysis and Modeling of Neural Systems Workshop, Berkeley, CA (in preparation).



- [2] Spence, C.D. and Pearson, J.C., "A resonance model of high frequency binaural phase sensitivity in the barn owl's auditory brainstem," *Proceedings of the Second Analysis and Modeling of Neural Systems Workshop, Berkeley, CA* (in press).
- [3] Spence, C.D. and Pearson, J.C., "A resonance model of microsecond time sensitivity in nucleus laminaris of the barn owl," *Society for Neuroscience Abstracts* **17** (124.20), 306 (1991).
- [4] Sullivan, W.E., "Possible mechanisms of high frequency phase comparison in barn owls," *Society for Neuroscience Abstracts* **17** (181.19), 447 (1991).
- [5] Sullivan, W.E., "Non-linear processes in binaural time comparison: Possible structure-function correlations in dendrites and axons and their implications for the origins of functional segregation and parallel processing," (in preparation, to be submitted to *Nature*).
- [6] Sullivan, W.E., "Modeling high frequency phase comparison in nucleus laminaris of the barn owl," (in preparation, to be submitted to the *Journal of Neuroscience*).

## V. PERSONNEL

The principle investigators are J. C. Pearson, Head, Computational Science Research, at the David Sarnoff Research Center and Professor W. E. Sullivan of the Biology Department of Princeton University; both institutions are located in Princeton, NJ. Dr. Pearson is the project director, and is also involved with research in the applications of artificial neural networks to signal processing problems. Dr. Sullivan, who is an experimental neuroscientist active in this field, serves as a consultant and ensures that the models developed at Sarnoff incorporate the latest findings and are biologically feasible and testable. Dr. Sullivan is also developing neurocomputational models related to the themes of this project. Working with Dr. Pearson at Sarnoff is Dr. C. D. Spence, Member of the Technical Staff.

## VI. INTERACTIONS

Communication with R. Adolphs, a graduate student in the Konishi Lab of CalTech, continued this year, as described in Section III-D.

We are planning a joint proposal with T. Takahashi at the University of Oregon to study the simultaneous processing of multiple sources of sound.

In July, Dr. Pearson gave an invited talk describing our models of elevation or intensity difference processing at the second "Analysis and Modeling of Neural Systems" workshop held in

San Francisco, CA. At the same conference, Drs. Pearson and Spence also presented a poster (paper in press, see Appendix B) about the laminaris analysis.

In November, Drs. Spence and Pearson presented a poster at the Society for Neuroscience meeting in New Orleans, LA.

## VII. REFERENCES

- [1] Spence, C.D. and Pearson, J.C., "A resonance model of high frequency binaural phase sensitivity in the barn owl's auditory brainstem," Proceedings of the Second Analysis and Modeling of Neural Systems Workshop, Berkeley, CA (in press).
- [2] Sullivan, W.E., "Modeling high frequency phase comparison in nucleus laminaris of the barn owl," (in preparation, to be submitted to the Journal of Neuroscience).
- [3] Pearson, J. C., Spence, C. D. and Adolphs, R., "The computation of sound elevation in the barn owl: model and physiology," Society for Neuroscience Abstracts **16** (299.3), 718 (1990).
- [4] Spence, C. D. and Pearson, J. C., "The computation of sound source elevation in the barn owl," Advances in Neural Information Processing Systems 2, edited by D. S. Touretzky (Morgan Kaufmann, San Mateo, CA, 1989), pp. 10-17.
- [5] Spence, C. D. and Pearson, J. C., "Models of the computation of sound elevation in the barn owl," Analysis and Modeling of Neural Systems, edited by F. Eeckman (Kluwer, Boston, MA, 1991), pp. 297-302.
- [6] Pearson, J.C., Spence, C.D. and Adolphs, R., "Model of the origin of neuronal selectivity for binaural intensity difference in the barn owl," Proceedings of the second Analysis and Modeling of Neural Systems Workshop, Berkeley, CA (in preparation).

APPENDIX A

**A resonance model of high frequency binaural phase sensitivity in the barn owl's auditory  
brainstem**

To appear in the proceedings of the conference

*Analysis and Modelling of Neural Systems II,*

San Francisco, California, July 1991

## A resonance model of high frequency binaural phase sensitivity in the barn owl's auditory brainstem

Clay Spence and John Pearson  
David Sarnoff Research Center  
CN5300  
Princeton, NJ 08543-5300  
e-mail: cds@sarnoff.sarnoff.com

### ABSTRACT

*The auditory system of the barn owl (*tyto alba*) contains neurons sensitive to the phase of sounds of remarkably high frequency, up to 9 kHz. Nucleus Laminaris represents phase differences as part of the computation of stimulus azimuth. The high frequency of the stimulus and the high level of noise in the input spike trains make the response properties of laminaris neurons hard to explain. We use simulations and semi-numerical analysis to show that the cellular and synaptic time constants must be unreasonably fast in order for ordinary biophysical mechanisms to reproduce the observed behavior. Several people have suggested that a resonance mechanism may exist in laminaris neurons to amplify the signal. We present a simple neuronal resonance model that can deal with realistic input.*

### INTRODUCTION

The barn owl (*tyto alba*) uses inter-aural phase difference as a cue for azimuth [Moiseff and Konishi, 1981; Moiseff, 1989]. At the neural level, action potentials in the eighth nerve, in the neurons of nucleus magnocellularis (NM), and in the neurons of nucleus laminaris (NL) are all phase locked to the stimulus [Sullivan and Konishi, 1984; Sullivan and Konishi, 1986]. They do not occur on every cycle of

## ANALYSIS AND MODELING OF NEURAL SYSTEMS II

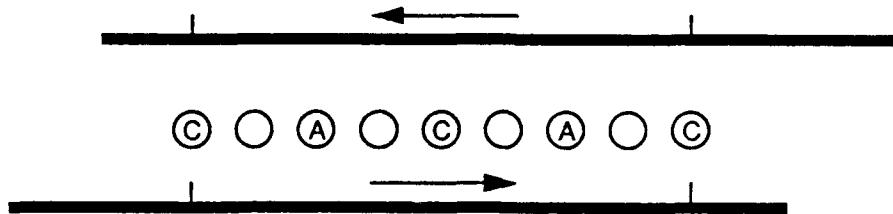


**Figure 1.** The Jeffress model. Circles labelled C and A represent neurons at coincident and anti-coincident positions for this stimulus condition. The heavy lines are axons with spike trains.

the stimulus, but a phase histogram shows a maximum at a particular phase and a minimum  $180^\circ$  from this phase. This phase sensitivity of the response decreases with increasing frequency, but is still present at nearly nine kHz. Nucleus magnocellularis (NM) receives synapses from the eighth nerve and is monaural. Axons from each NM innervate nucleus laminaris on both sides of the brain, penetrating the nucleus in opposite directions. NL neurons are sensitive to the binaural phase difference of the stimulus, showing a large response to a particular phase difference and very small response when the phase difference is  $180^\circ$  from the optimal, and in fact the response at this phase is less than the response to a monaural stimulus. There is evidence that the optimal phases of NL neurons vary systematically with their position, thus forming a map of inter-aural phase difference [Sullivan and Konishi, 1984; Carr and Konishi, 1988; Carr and Konishi, 1990].

Laminaris appears to be a perfect example of Jeffress' model for converting timing information at the ears into the azimuth of the source (Fig. 1) [Jeffress, 1948]. If a source of sound is to the right of the direction the animal is facing, its sound reaches the right ear before the left, and the difference of arrival times is a function of the azimuthal angle. In Jeffress' model, monaural neurons on each side of the head generate precisely timed action potentials in response to the sound. Thus the spike trains from each side of the head are very similar except for a relative time shift which reflects the azimuth of the source. These axons pass each other in opposite directions, making synapses onto binaural neurons. For each such neuron, there is an azimuth for which the difference in the time delays from a source to the ears is compensated by the difference in the neural time delays, so that the difference in the total time delays is zero. For this azimuth, spikes will arrive in coincidence at this neuron (a stimulus condition we will call in-phase). For the same stimulus, other neurons will have positions at which the spikes arrive first from one side and then the other, or in anti-coincidence (out-of-phase). If it can respond differently to coincident spike arrival than to anti-coincident arrival, the population of binaural neurons will form a map of inter-aural time difference and hence azimuth.

The essential features of the Jeffress model are the use of axons as delay lines and coincidence detection by binaural neurons. Although the evidence for the function of magnocellularis axons as delay lines is compelling, there is no real evidence that

## A RESONANCE MODEL IN THE OWL

laminaris neurons can detect the coincidence of action potentials. There is strong reason to believe that they cannot do this, simply because laminaris functions at up to nine kHz, which should exceed the speed limitations of an ordinary neuron. Also the jitter or imprecise timing of magnocellularis action potentials represents a source of noise which can swamp the signal that laminaris is trying to detect. We will analyze a single compartment model of a laminaris neuron to illustrate this. Such a model works only if the time constants for the synaptic conductances and the membrane potential are extremely fast, and then it works poorly.

As an alternative to coincidence detection, several people have suggested that a resonance mechanism of some sort may be present in NL neurons. This would serve to amplify the signal a laminaris neuron is trying to detect while suppressing the noise. As a preliminary model of a resonator, we show that a damped harmonic oscillator has the same response behavior as NL neurons to several types of stimuli: a large response to binaural in-phase stimuli, a smaller response to monaural stimuli, and very little response to binaural out-of-phase stimuli. We will present results showing that such a system can perform quite well, but good performance with reasonable synaptic and membrane time constants may require the cell's latency to be longer than is experimentally observed.

This work is still preliminary. In the last section we discuss the limitations of these models, and what remains to be done.

## LAMINARIS NEURONS ARE NOT COINCIDENCE DETECTORS: QUALITATIVE ARGUMENTS

In the simplest picture of a laminaris neuron as a coincidence detector, incoming spikes from nucleus magnocellularis excite the neuron. If the spikes occur in coincidence from each side of the brain, the excitation is relatively large, whereas if the spikes are anti-coincident, their effects do not add as effectively, and so the excitation is relatively small. One would only need to set a threshold to distinguish between the two stimulus conditions. However, there are laminaris neurons with best frequencies of around nine kHz. Synaptic and membrane time constants are usually thought to be on the order of one millisecond, so a typical neuron would badly smear signals with a frequency greater than about one kHz.

If the input to a laminaris neuron had no noise the membrane potential would have a DC component and a very small component following the input signal. A thresholding mechanism could still work if the threshold could be adjusted with sufficient accuracy. However, the input to laminaris is noisy. The magnocellularis neurons providing this input show little or no modulation of their firing rates with stimulus intensity, but phase lock to the stimulus. They do not fire spikes at exactly the same phase of the stimulus, rather the spikes are spread over some range of phases. Furthermore, they do not fire during every period of the stimulus, nor are their spikes spaced by a predictable number of stimulus periods. This randomness in the occurrence of spikes represents noise in the input to each laminaris neuron.

## ANALYSIS AND MODELING OF NEURAL SYSTEMS II

One might imagine that by making the synaptic and membrane time constants short enough the modulation of the spike rate will become detectable by the cell. This may require the time constants to be unreasonably fast. A more basic problem with this picture is that it does not really cure the noise problem. Because the stimulus period is so short, only a few spikes arrive during one such period on average, and the fluctuation in the number of spikes arriving is substantial, unless magnocellularis neurons communicate with each other so that the average number firing in a given period does not fluctuate much, a possibility which we think is unlikely.

### THE SIGNAL-TO-NOISE RATIO IN LAMINARIS

To give a more quantitative analysis of the problem, we will estimate the mean squared amplitude of the noise fluctuations and of the signal in the membrane potential of a single compartment model of a laminaris neuron. We model the input to a laminaris neuron as a Poisson process  $\xi(t)$  whose rate is modulated sinusoidally. (A periodic but non-sinusoidal modulation will not give better performance in a linearized model, since it differs from a sinusoidal modulation only by having non-zero harmonics of the fundamental frequency. These higher frequencies are suppressed even more than the fundamental.) In the in-phase condition the modulation is maximal, so  $\xi$  has average

$$\langle \xi(t) \rangle = R(1 + \cos(\Omega t + \varphi)) \quad 1$$

where  $\varphi$  is a random phase,  $R$  is the long-time-averaged rate and  $\Omega$  is the (angular) stimulus frequency. The auto-correlation function is

$$\begin{aligned} \langle \xi(t + \tau) \xi(t) \rangle &= R^2(1 + \cos(\Omega(t + \tau) + \varphi))(1 + \cos(\Omega t + \varphi)) \\ &\quad + R\delta(\tau)(1 + \cos(\Omega t + \varphi)) \end{aligned} \quad 2$$

Averaged over  $\varphi$ , this gives

$$\langle \langle \xi(t + \tau) \xi(t) \rangle \rangle_{\varphi} = R^2\left(1 + \frac{1}{2}\cos(\Omega\tau)\right) + R\delta(\tau) \quad 3$$

The mean square fluctuation of a stochastic process is given by the total power of the process, so we would like the power spectrum of the model input process. The power spectrum of this process is (taking the Fourier transform)

$$P(\omega) = R + R^2\delta(\omega) + \frac{R^2}{4}(\delta(\omega - \Omega) + \delta(\omega + \Omega)) \quad 4$$

The first term is noise and is present at all frequencies. The second term represents a DC offset. The third term is the signal. Notice that the total power in the noise is infinite.

The model neuron's membrane potential obeys the equation

$$C \frac{dv}{dt} = -g_L(v - v_L) - g_E(v - v_E) \quad 5$$

## A RESONANCE MODEL IN THE OWL

where  $C$  is the membrane capacitance,  $g_L$  and  $v_L$  are the constant leakage conductance and reversal potential,  $g_E$  is the excitatory synaptic conductance, and  $v_E$  is the constant excitatory reversal potential. The response of  $g_E$  to a spike is just the commonly used function  $Ate^{-\gamma_s t}$  [MacGregor, 1987]. The response of  $g_E$  to several spikes is just the sum of the responses to individual spikes. This gives  $g_E$  the value

$$\int_{-\infty}^t ds A \cdot (t-s) e^{-\gamma_s(t-s)} \xi(s) \quad 6$$

The conductance response to the spike train is just a linearly filtered version of it. The power spectrum of the conductance is the power spectrum of the input multiplied by the squared-amplitude of the fourier transform of the response of the conductances impulse response, which is

$$\frac{A^2}{(\omega^2 + \gamma_s^2)^2} \quad 7$$

The equation for the membrane potential is non-linear, but for time constants which are not too fast the fluctuations in the membrane potential are small compared to the DC offset, so we can linearize about the constant parts of the potential and synaptic conductance. Denoting the fluctuating part of the potential by  $u$ , we get

$$C \frac{du}{dt} + g_L u + G_E u + g_E (U - v_E) = 0 \quad 8$$

where the capital letters denote constant parts and small letters denote the fluctuating parts. The impulse response of  $u$  to  $g_E$  is

$$\frac{(U - v_E)^2 / C^2}{\omega^2 + \left(\frac{g_L + G_E}{C}\right)^2} \quad 9$$

$(g_L + G_E) / C$  is just the inverse of the average time constant of the membrane potential, so we will call it  $\gamma_C$  in what follows. Thus the power spectrum of the noise in the membrane potential is

$$\frac{RA^2 (U - v_E)^2 / C^2}{(\omega^2 + \gamma_s^2)^2 (\omega^2 + \gamma_C^2)} \quad 10$$

The total power is

$$\int \frac{d\omega}{2\pi} \frac{RA^2 (U - v_E)^2 / C^2}{(\omega^2 + \gamma_s^2)^2 (\omega^2 + \gamma_C^2)} = \frac{RA^2 (U - v_E)^2}{C^2} \times \frac{\gamma_C + 2\gamma_s}{4\gamma_C \gamma_s^3 (\gamma_C + \gamma_s)^2} \quad 11$$

The total power of the signal in the membrane potential is trivial to evaluate



## ANALYSIS AND MODELING OF NEURAL SYSTEMS II

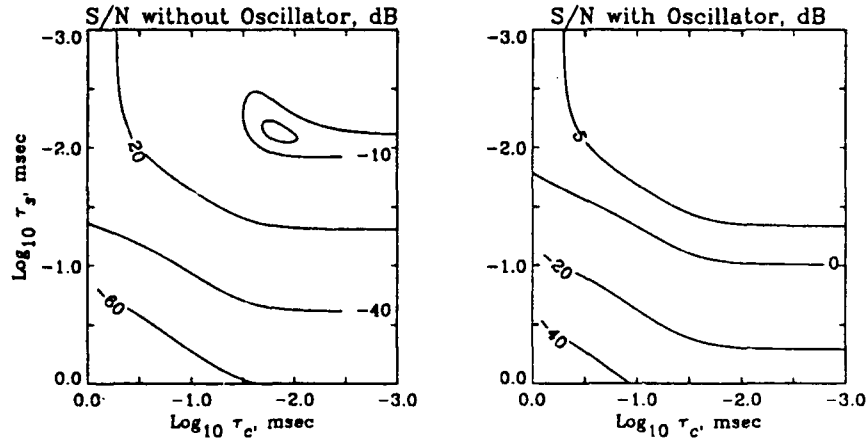


**Figure 2.** The signal-to-noise ratio of a passive compartment as a function of the synaptic and membrane time constants. Note the maximum without an oscillator.

because of the delta-functions. It is

$$\frac{A^2 R^2 (U - v_E)^2 / C^2}{4\pi (\Omega^2 + \gamma_S^2)^2 (\Omega^2 + \gamma_C^2)} \quad 12$$

The signal-to-noise ratio is

$$\frac{R\gamma_C\gamma_S^3(\gamma_C + \gamma_S)^2}{\pi(\gamma_C + 2\gamma_S)(\Omega^2 + \gamma_S^2)^2(\Omega^2 + \gamma_C^2)} \quad 13$$

Figure 2 is a contour plot of the signal-to-noise ratio versus  $\gamma_C$  and  $\gamma_S$ , with  $\Omega = 2\pi \times 5$  kHz, and  $R = 30$  spikes per msec (100 synapses times 0.3 spikes per msec per synapse). Note that the function has a maximum. The signal-to-noise ratio there is -9.6 dB. Furthermore, this maximum occurs for  $\gamma_C^1 = 0.015$  msec and  $\gamma_S^1 = 0.0074$  msec, which we think are unreasonably small.

### RESONATORS IN LAMINARIS NEURONS?

A resonator can help a laminaris neuron by suppressing the noise while amplifying the signal. A linear resonator has some of the response properties of a laminaris neuron:

Real laminaris neurons have a binaural response that is roughly a sinusoidal function of the phase difference. In a resonator model, the average input spike rate is the sum of two periodic signals. The amplitude of the modulation at the stimulus frequency is a smooth function of the phase difference, and so the response of a linear filter at this frequency will also be a smooth

## A RESONANCE MODEL IN THE OWL

function of the phase difference.

Real laminaris neurons have a monaural response that is roughly half of the in-phase binaural response. In a resonator model, the input spike rate would have two pieces: a constant piece due to the unstimulated ear and a maximally modulated piece from the stimulated ear. The modulation of the total rate at the stimulus frequency has half of the amplitude of the in-phase binaural stimulus condition, so a linear filter will also have half of the response at the stimulus frequency.

A simple and familiar model of a resonator is a damped harmonic oscillator. The oscillator's response at the resonance frequency can be made arbitrarily large, but at the cost of increasing the time it takes for the oscillator to reach its steady-state response. This means a oscillator model neuron could have an unacceptably long latency.

We repeat the same calculations as the last section, except with the cell voltage driving a damped harmonic oscillator. In the simplest model, there is no feedback to the cell voltage. So we have simply added an extra equation,

$$\frac{d^2q}{dt^2} + \gamma_0 \frac{dq}{dt} + \Omega^2 q = Bv \quad 14$$

The power spectrum of  $q$  is just the power spectrum for  $v$ , but with the additional factor

$$\frac{B^2}{(\omega^2 - \Omega^2)^2 + \gamma_0^2 \omega^2} \quad 15$$

In principle, the resulting power spectrum can also be integrated, but it is more tedious than the case without the oscillator, so we have computed the total power by integrating the power spectrum numerically. Since the damping constant  $\gamma_0$  is the inverse of the oscillator's latency, we choose the constant to be one kHz. The results are shown in figure 2. Obviously, the oscillator improves the performance quite a bit, but for this value of  $\gamma_0$  the synaptic and cellular time constants must still be rather short.

## SIMULATIONS

In sections 3 and 4, we had to use very fast time constants in order to get acceptable behavior from the model neuron. At very fast time constants, the linear approximation used breaks down, so one might question the relevance of the results. Also, while the signal-to-noise ratio may give the relative magnitudes of the signal and noise fluctuations, this is still not the same as spike rates. In this section we present the results of simulations of the model laminaris neuron, with and without the harmonic oscillator.

The differential equations for the membrane potential (without linearizing it) and

## ANALYSIS AND MODELING OF NEURAL SYSTEMS II

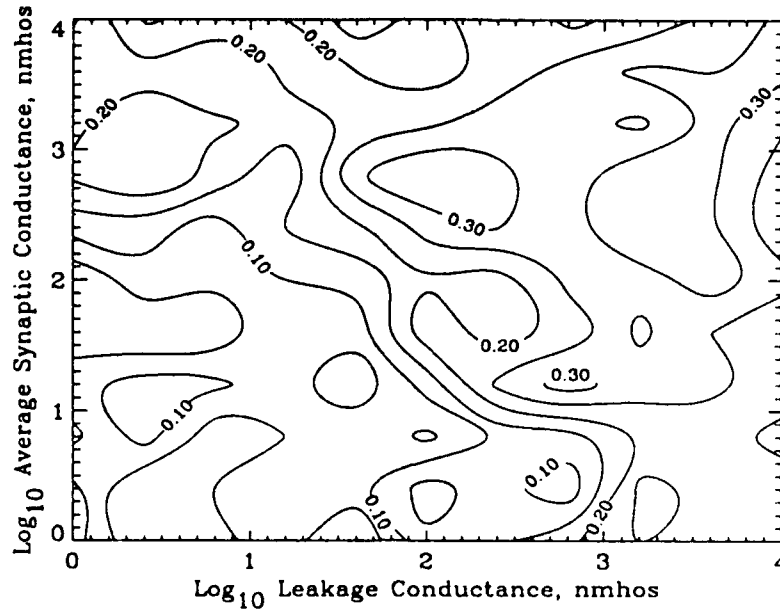


**Figure 3.** Rate difference between the in-phase and out-of-phase stimulus conditions from a simulation of a passive compartment model. The rate difference is expressed as a fraction of the maximum possible firing rate. The synaptic time constant was 0.01 msec.

the oscillator were integrated in time steps much shorter than the stimulus period or any of the time constants. The synaptic conductance obeys the equation for a critically damped harmonic oscillator driven by the input spikes:

$$\frac{d^2 g_E}{dt^2} + 2\gamma_S \frac{dg_E}{dt} + \gamma_S^2 g_E = A\xi(t) \quad 16$$

A input spike just increments  $dg_E/dt$  by  $A$ . This is just a convenient way of realizing equation 3.6. Spikes only arrived at the beginning of time steps. Each independent variable's differential equation was integrated by using the exact expression for the solution of the same equation with the other variables held constant. An action potential was considered to be generated when the membrane potential exceeded a fixed threshold, or when the oscillator coordinate  $q$  exceeded a threshold in the model with an oscillator. The threshold which gave the largest difference in the firing rate in a 100 msec interval was used. The cell's capacitance was 30 pF (from a specific capacitance of  $1 \mu\text{F}/\text{cm}^2$  and a cell diameter of  $30 \mu\text{m}$ ). The upper limits were chosen to give similar time constants as in figure 2. For comparison, note that if the soma had a high density ( $500/\mu\text{m}^2$ ) of sodium channels as in the Hodgkin-Huxley model and all of them were open (conductance  $\sim 0.01 \text{ nmho}$ ), the conductance would be about 50000 nmho, giving a time constant of about

## A RESONANCE MODEL IN THE OWL

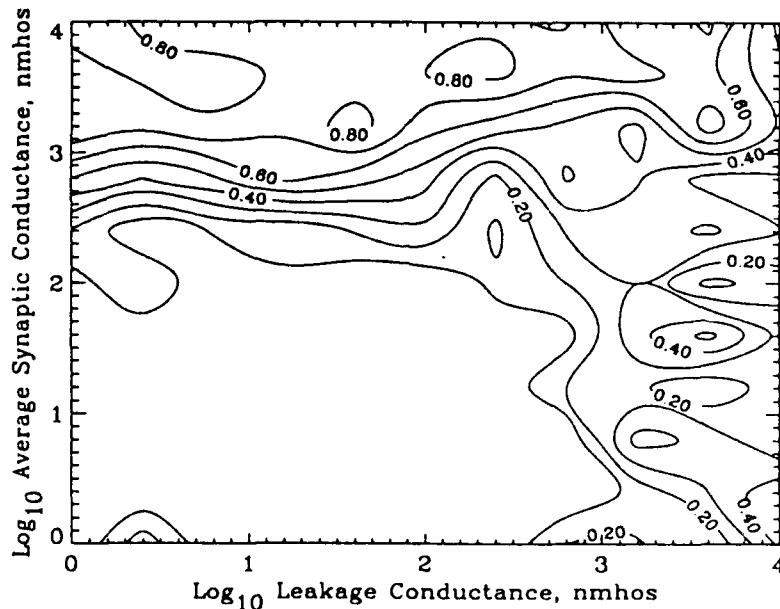


**Figure 4.** Rate difference between the in-phase and out-of-phase stimulus conditions from a simulation of a passive compartment model driving a damped harmonic oscillator. The rate difference is expressed as a fraction of the maximum possible firing rate. The synaptic time constant was 0.25 msec.

0.0006 msec. Figures 3 and 4 show the resulting difference between the in-phase and out-of-phase firing rates, shown as a fraction of the maximum firing rate. Without an oscillator, the rate difference is significant, but only at very high conductance values. With an oscillator there is substantial improvement, but it is still questionable whether a neuron can have such high conductances and short synaptic time constants.

### CONCLUSIONS AND FUTURE WORK

We have presented the results of calculations of a passive single compartment model for a laminaris neuron. The results show that such a model cannot work at the high frequencies and noise levels which are typical of the input to a laminaris neuron. Faster time constants for the synaptic conductance and membrane potential cannot cure the problem, which arises from the noisy nature of the input. There must be some mechanism for filtering the neuron's input to suppress the noise relative to the signal. We have also presented calculations for a resonance model of such filtering. This model has substantially improved performance, and in fact can work well if the synaptic and membrane time constants are fast enough. It can work well even if those time constants are slow, but only by increasing the latency of the cell's response.

## ANALYSIS AND MODELING OF NEURAL SYSTEMS II

Part of the purpose of this work was to determine if ordinary neuron models can show behavior similar to that of a laminaris neuron. There are several fairly conventional changes to these models which could improve their performance. One such change would be an adaptive effective threshold. This would suppress low frequency components in the input, thereby raising the signal-to-noise ratio. Active channels as in the Hodgkin-Huxley model could do this, or one could use a simpler model like Hill's [Hill, 1936]. Another change of the model which could improve its performance would be a more realistic input spike train model. The Poisson process model of the input is the noisiest possible choice, and is almost certainly noisier than the actual input. For example, the refractory periods of magnocellular neurons prevent more than a certain number of spikes from arriving at laminaris in a given interval. There may also be a lower limit on the number of spikes which can arrive in a given interval, if magnocellular neurons can't go longer than a certain interval without spiking. These properties are not true of a Poisson process, and may reduce the noise.

There is also the question of the biophysical mechanism of such high-frequency resonance. Active channels can show behavior similar to resonance, but they are normally thought to respond too slowly. In addition, they would form a non-linear system whereas laminaris at least shows hints of being linear in the magnitude of the modulation of the input firing rate. Hudspeth proposed a resonator model of cochlear hair cells [Hudspeth, 1985]. However, this model requires different external ionic concentrations on different parts of the resonating cell's membrane. The structure of laminaris gives no hint that it can maintain such differences. Also, Hudspeth's model operates at very low frequencies, on the order of one hundred Hertz.

We do not yet have a mechanism to suggest, we can only say that some enhancement of the signal relative to the noise is necessary. In order to make further progress, the resonator hypothesis needs to be tested experimentally. The voltage response to step current injections and/or sinusoidal current injections at various amplitudes and frequencies around the neuron's best frequency should reveal the presence of a resonator and provide insight into its mechanism, if in fact a resonator is found.

### ACKNOWLEDGMENTS

This work was supported by AFOSR contract F49620-89-C-0131 and DARPA contract F49620-90-C-0010.

### REFERENCES

- Carr, C.E. and M. Konishi (1988). Axonal delay lines create maps of interaural phase difference in the owl's brainstem. *Proc. Natl. Acad. Sci. USA* 85:8311-8315.
- Carr, C.E. and M. Konishi (1990). A circuit for detection of interaural time differences in the brainstem of the barn owl. *J. Neurosci.* 10:3227-3246.

## A RESONANCE MODEL IN THE OWL

Hill, A.V. (1936). Excitation and accommodation in nerve. *Proc. R. Soc. London, Ser. B*, 119:305-355.

Hudspeth, A.J. (1985). The cellular basis of hearing: the biophysics of hair cells. *Science*, 230:745-752.

Jeffress, L.A. (1948). A place theory of sound localization. *J. Comp. Physiol. Psychol.* 41:35-39.

MacGregor, R.J. (1987). *Neural and Brain Modelling*. Academic Press, San Diego.

Moiseff, A. and M. Konishi (1981). Neuronal and behavioral sensitivity to binaural time differences in the owl. *J. Neurosci.* 1:40-48.

Moiseff, A. (1989). Bi-coordinate sound localization by the barn owl. *J. Comp. Physiol.* 164:637-644.

Sullivan, W.E. and M. Konishi (1984). Segregation of stimulus phase and intensity coding in the cochlear nucleus of the barn owl. *J. Neurosci.* 4: 1787-1799.

Sullivan, W.E. and M. Konishi (1986). Neural map of interaural phase difference in the barn owl's brainstem. *Proc. Natl. Acad. Sci. USA* 83:8400-8404.

APPENDIX B

**Modeling high frequency phase comparison in nucleus laminaris of the barn owl**

in preparation,

to be submitted to the Journal of Neuroscience

Modeling high frequency phase comparison in nucleus laminaris of the barn owl.

W. Edward Sullivan

Department of Ecology and Evolutionary Biology  
and  
Program in Neuroscience  
Princeton University, Princeton, N.J.

To be submitted to  
J. Neuroscience



## Abstract

The horizontal localization of sounds by measurement of interaural time difference involves a system of neural "delay-lines" and binaural "coincidence detectors" (Jeffress 1948). This study explores the biophysical problems inherent in high frequency phase processing by barn owls to gain new insights into possible mechanisms of coincidence detection. The analyses show that both the time course of synaptic transmitter release and the biophysics of spike generation can play important roles in producing a phase discriminant spike output for high frequency inputs.

The "input" to a neuron is the spatial-temporal conductance pattern evoked by its afferent synapses. Simulations of conductance patterns produced by many phase-locked cochlear nucleus axons synapsing onto the soma and short somatic spines of a barn owl laminaris neuron, show that conductance is modulated at the stimulus frequency when all input axons are coherently phase-locked. The relative strength of this modulation depends on the shape and duration of individual conductance changes, on the number of converging inputs and on the relative phase of bilateral inputs, being maximal for in phase stimulation and absent for out-of-phase stimulation. Greater synaptic durations produce a larger amount of random variation in synaptic input relative to the stimulus dependent signal and a larger background of continuous excitation.

Simulations of spike output using modifications to the Hodgkin-Huxley model show that a robust, discriminatory response can be achieved with either brief or long synaptic durations, but that the parameters required for spike generation depend on the characteristics of the synaptic input. The weaker phase-dependent conductance signal and larger background excitation produced by long synaptic durations can be compensated by increases in voltage sensitive channel density and activation rate either alone or in combination with a larger leakage conductance and/or steady inhibition. Inhibition may also be important in compensating for increases in excitatory input level to produce a response whose magnitude is affected only by relative phase. Finally, voltage sensitive potassium channels were found to enable a response to high frequency, phase dependent modulations in preference to the random modulations of lower

frequency, suggesting a model for coincidence detection involving frequency filtering or resonance rather than simple threshold detection (Spence and Pearson 1991).

The results suggest that specializations of both synaptic input and spike output can enable phase discrimination at high frequencies. This, in addition to further sharpening at higher levels in the auditory pathway, obviates the necessity for extremely large changes in any one parameter.

### **Introduction:**

Although the computation of horizontal sound location commonly involves measurements of binaural differences in waveform timing (or phase), the barn owl is thought to be unique in its ability to use high frequency sounds for this purpose (Moiseff and Konishi 1981). In birds, neural sensitivity to binaural phase difference is generated in nucleus laminaris, the avian analog of the medial superior olivary nucleus (Moiseff and Konishi 1983, Young and Rubel 1983, Sullivan and Konishi 1986, Carr and Konishi 1988,1990, Overholt et.al. 1992). Cells in this nucleus receive phase-locked synaptic inputs from each magnocellular cochlear nucleus and can respond both to monaural and binaural stimulation (Sullivan and Konishi 1984, Takahashi and Konishi 1988). The binaural response is sensitive to interaural time difference or ITD (Sullivan and Konishi 1986, Carr and Konishi 1988, 1990), such that a cell's best ITD occurs when the inputs from the two sides are coherent. This suggested that laminaris neurons act as coincidence detectors in the sense that simultaneous inputs from the two ears are necessary for a maximal response (Jeffress 1948).

While phenomenological evidence in favor of Jeffress' "delay-line / coincidence detector" model is quite strong, little is known about the actual biophysical mechanisms by which coincidence detection is achieved, especially at frequencies whose period is much less than a millisecond. The simplest coincidence model assumes that each synaptic input is subthreshold so that two, nearly simultaneous inputs are required to cause an output. However, this does not take into account the high

sound frequencies and large degree of convergence which together subject barn owl laminaris neurons to a continuous bombardment of synaptic inputs. That is, rather than selecting on the basis of one vs. two synaptic events, laminaris neurons must be sensitive to differences in synaptic pattern which distinguish in-phase from out-of-phase arrival of a large number of synapses from the two sides. The purpose of the present study is to explore possible mechanisms of coincidence detection in the barn owl by simulating both synaptic input patterns and spike generation processes. What emerges from these analyses is the conclusion that both mechanisms to control the shape and duration of synaptic input and to produce spike output can contribute to high frequency phase selectivity, and that the changes required to produce this selectivity are not unreasonably large. Since further sharpening of ITD tuning occurs after its generation in laminaris (Fujita and Konishi 1991), it is likely that the dramatic improvements in localizing high frequency sound by phase comparison seen in the barn owl are due to numerous, but less dramatic changes at many points along the time pathway. The analyses also suggest that the simple threshold model should be modified in favor of a model that selects both on the amplitude and rate of change of synaptic inputs.

The simulations are organized into three major phases as shown in figure 1. First, stochastic spike trains possessing interspike interval and period histogram statistics similar to those of magnocellular afferents are constructed by a pseudorandom process. Next, these spike trains are used to compute synaptic conductance functions using variable assumptions about the shape and duration of individual post-synaptic conductance changes. Synaptic conductance is chosen as an intermediary since it represents the actual input to the laminaris cell and unlike current and voltage is assumed not to be a function of the post-synaptic cell's membrane properties ( a safe assumption if channels such as NMDA receptors are not involved). Amplitude and spectral analysis of this "conductance signal" suggest some ways in which choices of synaptic conductance functions affect the discrimination problem faced by the laminaris cell. Third, this synaptic conductance signal is used as the input to a biophysical model of the laminaris cell employing the Hodgkin-

Huxley model of action potential generation to which parameter modifications are applied.

#### Modeling the laminaris synaptic input:

The properties of magnocellular spike trains suggest that they can be modeled as a stochastic process in which firing probability is sinusoidally modulated (Molnar and Pfeiffer 1968). As shown in figure 2, for every time step (10  $\mu$ sec), a pseudo-random number is generated which produces a "spike" if this number exceeds a sinusoidally modulated threshold value. Each spike is followed by an absolute refractory period (where threshold is infinite) and a relative refractory period in which threshold falls exponentially to its resting value.

As shown in figure 3, this process produces an interspike interval histogram resembling a Poisson distribution. When compared to data obtained from magnocellular units however, this simple procedure produces unrealistic results. If the relative refractory period chosen is relatively short, the peak of the interspike histogram can be approximately matched, but the artificially generated ISI falls off much more rapidly than the real histogram. Conversely, if the relative refractory period is greater, both the peak and the tail of the histogram are not properly matched. It appears therefore that magnocellular units have too many long interspike intervals relative to their peak interval to be matched by this procedure. This observation led to the hypothesis that short interspike intervals may tend to be followed by long interspike intervals and vice versa. That is, if a cell has fired two spikes in rapid succession, it may have built up refractoriness such that it will tend not to fire for a greater period. In contrast, if a cell had fired after a long interspike interval, it is assumed to have recovered enough to be capable of producing a much shorter interval with the next spike. The feasibility of this hypothesis was verified by modifying the simulation such that the rate of exponential recovery during the relative refractory period was made to be contingent upon the last interspike interval. To do this, a reference interval was chosen and was divided by each spike interval so that a short interval produces a large ratio and a large interval a small

The effects of synaptic duration are shown graphically by comparing conductance patterns produced by short and long durations (fig. 4 and 5 respectively). Figure 4 shows the conductance patterns and frequency spectra computed for a fairly long synaptic duration. (This consists of the "alpha" function defined by Rall 1969 as  $t/T e^{(1-t/T)}$  in which the time constant  $T$  is 150  $\mu$ sec. This function has a start to finish duration of about 1 msec and a 1/2 width of 367  $\mu$ sec.) The resulting conductance patterns computed for in-phase and out-of-phase conditions have similar peak-to-peak amplitudes and a substantial offset bias. The major difference between the two is in their spectral content, with the in-phase pattern containing a modulation at the "stimulus" frequency (i.e. the modulation frequency used to create the input spike trains). In contrast, if a much shorter synaptic duration is employed as in fig. 5 (alpha time constant = 20  $\mu$ sec), the in-phase signal has a clearly larger peak-to-peak amplitude and both patterns have a small offset. The spectral differences between the two patterns are also greater as shown by Fourier analysis.

The effects of the arbitrary choices of synaptic shape and duration were examined by varying these over a wide range and computing the resulting S/N ratio of the resulting synaptic waveforms. The "signal" strength was taken as the peak of the Fourier power spectrum for the in-phase condition and the "noise" was measured by computing the sum of squared deviations from the mean of the signal computed for the out-of-phase condition, since it is the former which the laminaris neuron must detect and the latter that must be rejected. As shown in figure 6, the exact shape of the synaptic conductance function appears to have little significance while the duration (measured by the time delay between 50% crossings of the rising and falling phases) of the individual synaptic conductance change has a significant effect. Signal-to-noise ratio is maximal for synaptic durations of approximately 1/2 the duration of the original "stimulus" period which was 200  $\mu$ sec in these simulations, and at this peak, signal-to-noise seems to be independent of shape.

A further analysis at higher synaptic durations suggests that the rise time of the synaptic function controls the size of the 5 kHz stimulus

dependent signal while its overall duration controls both the size of the noise signal and of the sustained excitatory offset (fig. 7). Figure 7a plots the size of the in-phase stimulus signal as a function of overall synaptic duration given constant rise time. This value reaches a peak at 1/2 of the stimulus period but for long durations it remains essentially constant. The mean squared deviation of the out-of-phase signal continues to build as duration increases (fig 7b). This is most likely due to the fact that longer durations enable a greater accumulation of errors in that aberrant spikes have a lingering influence on the synaptic pattern. Note that the size of this random signal becomes smaller relative to the size of the sustained offset component (which increases linearly with duration) but is larger with respect to the (constant) in-phase signal, and it is this latter comparison which is crucial in understanding the laminaris cell's discrimination problem.

In addition to synaptic duration and time course, the number of synaptic inputs (or convergence ratio) to a single laminaris cell is an important factor in determining how the amplitude and spectral properties of synaptic input change with interaural time delay. As shown in figure 8, increases in convergence ratio cause the synaptic ensemble calculated for coherent inputs to increase in magnitude relative to that calculated for out of phase inputs. Interestingly, improvements in signal-to-noise show diminishing returns after more than 200 to 300 inputs (fig. 8b), which is close to the convergence ratio estimated by Carr (personal communication). It is also interesting to note that improvements in signal-to-noise ratio with increases in synaptic convergence are most prominent at the peak of the duration curve, where S/N ratio is already optimized. For long synaptic duration, there appears to be less improvement with increased averaging and most of the improvement that is seen occurs as N is initially increased (see figure 8b), so that S/N ratio reaches its asymptotic value at these durations for convergence ratios of 100 or less. This would suggest that long synaptic durations are detrimental both because of their inherently poor S/N properties and because this low S/N is resistant to averaging. This property is probably related to the high coefficient of variation in the interspike intervals of the magnocellular inputs (Sullivan 1985 and above).

## Models of laminaris output: General considerations

An understanding of the synaptic input is quite important because it will affect the type of spike mechanism needed to discriminate between the input patterns associated with different phase conditions. As shown above, input analysis suggests that the synaptic conductance pattern will contain a phase-dependent modulation at the stimulation frequency as well as random fluctuations at lower frequencies. To perform its function, a laminaris neuron must respond selectively to this phase-dependent signal. This implies first that high frequency modulations are not removed by post-synaptic membrane filtering and secondly that the phase-dependent signal causes a response above that due to the noise. If signal-to-noise ratio is sufficient, a simple threshold spike model should enable reasonable interaural phase discrimination. However, with longer synaptic durations (which seem more feasible), amplitude differences will be small whereas spectral differences can still provide a reasonable basis for discrimination. Therefore, if laminaris neurons act as frequency tuned filters or resonators, they could respond preferentially to the in-phase conductance signal even if synaptic durations are in the millisecond rather than the microsecond range.

To explore possible spike output mechanisms, a standard model of action potential generation (Hodgkin and Huxley 1952) was employed (see Appendix I). Using the synaptic conductance patterns previously computed, spike outputs were calculated with different combinations of voltage sensitive channel densities, activation rate constants and excitatory and inhibitory conductances, to find those regions of parameter space capable of producing a selective response to the in-phase synaptic signal. The numerical simulations employed a Fourth-order Runge-Kutta algorithm with an adaptive time step (Press et.al. 1988). The input for these simulations was calculated for a 5 kHz, stimulus with 200 inputs from each side.

As shown in figure 9, given the assumption of relatively long synaptic duration and thus a poor input signal-to-noise ratio, parameter

combinations can still be found for which a strong response is only seen with phase coherent synaptic inputs over a wide range of synaptic conductance. Other parameter combinations produce large responses for both in- and out-of-phase inputs (fig. 10) or for neither. A strong but indiscriminate response can either be due to loss of the high frequency synaptic signal by post-synaptic filtering or to a spike generating process which is non-selective by virtue of being too easily triggered. In general, models which respond well both to correlated and uncorrelated inputs have sustained responses to constant excitation (fig. 10) whereas selective models respond transiently (fig. 9). The transient response is not however synonymous with good selectivity for input coherence, since models which are insensitive to either condition also display a transient response. Selective models have the ability to respond to the rapid modulations present in correlated inputs but not to the slower fluctuations and/or steady excitation seen with uncorrelated inputs. Voltage sensitive potassium channels appear to be critically important for this latter property.

To quantify the discriminative properties of a model, the total number of spikes evoked over the model's sensitive range (see below) was computed for both the in-phase and out-of-phase input conditions. These values were entered into the formula:  $1.0 - [\text{Sum of spikes for out-of-phase input}] / [\text{Sum of spikes for in-phase input}]$ . If as in figure 10, the cumulative spike counts for these two conditions are similar, the ratio of Out/In is close to 1.0 and the above difference is near 0.0. Conversely, if the response to the in-phase condition is much greater than the response to the out-of-phase input (as in figure 9), the Out/In ratio is near 0 and the difference near 1. This "phase discrimination index" thus provides a measure of the modulation depth in spike rate that a laminaris output cell would produce. As shown in figures 11 and 12, this discrimination index was computed for different combinations of sodium and potassium channel gating rates and as shown in figure 13, contour plots of discrimination index as functions of gating rate were computed for a number of different channel densities using both long and short duration synaptic inputs.



Analysis of results obtained with different combinations of voltage sensitive sodium and potassium channel densities and activation rates suggest that all of these factors are important in achieving phase selectivity at high frequencies. In all simulations (see figures 9 through 12), there is a range of synaptic conductance within which sustained activity is seen. Below this range, the input fails to achieve threshold and above this range, the model is held in a refractory state (Holden and Yoda 1981). Models with fewer voltage sensitive channels are more easily depolarized into this refractory range and can therefore be activated only by low synaptic conductances. Since membrane time constant is inversely proportional to conductance, the low conductances required for impedance matching prevent the membrane voltage from responding to rapid input modulations. Decreasing membrane time constant by increasing leakage conductance or adding steady inhibition in these models creates a different impedance matching problem because the inhibitory conductances create too large of a load on spike generation and the model becomes unresponsive. Finally, isolating the spike generator by putting it in the axon rather than the soma reduces the load on spike generation and increases threshold (thus enabling higher synaptic conductances to be used), but trades one form of low-pass filtering for another (unpublished observations). Thus, it seems clear that given a low input signal-to-noise, responsiveness to high frequency synaptic inputs requires large voltage sensitive conductances (as discussed below, this is more feasible biophysically than it is to consider large decreases in membrane capacitance).

If the density and/or activation rate of sodium channels is too high relative to that of potassium channels, discrimination between phase coherent and random inputs is poor because spikes are too easily triggered. In contrast if potassium channel density and/or rate constant is too high, there is no response to any input and no discrimination as well. As shown in figures 11 and 13 (right), discrimination between in-phase and out-of-phase inputs is maximized when these two voltage sensitive currents are large enough and properly balanced in terms of their relative density and activation kinetics. Voltage sensitive K<sup>+</sup> channels eliminate responses to slow modulations while leaving

responses to rapid modulations intact. Potassium channels thus perform a high-pass filtering function which boosts the relative influence of the high frequency information bearing conductance signal over that of lower frequency noise.

The balance between the voltage sensitive sodium and potassium currents needed for maximal discrimination can be achieved with a number of combinations of relative channel density, activation rate and leakage conductance. However, while the effects of increasing voltage sensitive conductances and activation rate constants are similar, they are not identical. First of all, changes in rate constants do not affect impedance matching. Thus, at low channel densities, increases in the activation speed of sodium and potassium channels do not make the model sensitive to rapid modulations because the model's behavior is limited by its membrane time constant (fig. 13, bottom right). The explosive positive feedback loop leading to an action potential contains two steps, one in which the present sodium conductance causes membrane depolarization and the second in which the new voltage causes activation of more sodium channels. Channel density affects both of these steps while activation rate affects only the second. At low channel densities, the speed of this loop is limited by the conductance-to-voltage step and no increase in channel rate can affect this limit. Increases in channel density bring about improvements in high frequency response both by producing smaller time constants and by enabling faster channel kinetics to be employed (figure 13, top right).

The previous results were obtained with input ensembles computed assuming a fairly long synaptic duration. If the much shorter, optimal synaptic duration is chosen, similar performance can be achieved with fewer voltage sensitive channels (figs. 12 & 13 left). These models still benefit from the effects of voltage sensitive potassium channels which if too numerous or too fast, shut off spike output and if too scarce or too slow, enable significant responses for both in-phase or out-of-phase input ensembles. In fact, with a highly modulated signal as produced by brief synaptic inputs, optimal phase discrimination performance is observed when potassium channel activation is slightly faster than sodium channel

activation, the reverse of what was seen with the longer synaptic duration. However, with the greater signal-to-noise ratio and lower steady excitation bias seen with short synaptic durations, higher channel densities are less important because the strong in-phase signal is still significant even after post-synaptic electrical filtering. A comparison of the parameters required for high frequency coincidence detection, must in part be determined by pre-synaptic mechanisms.

Inhibition - with high density, greater leakage or inhibitory conductance and enable good discrimination with slower activation rates.. Inhibition can also compensate for changes in average firing rate so that output is more closely related to phase difference ...

### **Discussion:**

Phase comparison at high frequencies undoubtedly involves a number of anatomical and physiological specializations, some to ensure that information at the frequency of interest is present in the synaptic input and others to enable that information to be processed. Ideally, the synaptic input to a laminaris cell should convey the temporal properties of each monaural stimulus while minimizing noise. This can be achieved by increasing the number of converging inputs and by decreasing the duration of each synaptic conductance change. If these input specializations are of sufficient magnitude, subsequent filtering other than threshold crossing detection at the laminaris spike output may be unnecessary. However, the laminaris cell must still contain some specializations to prevent it from filtering out the high frequency information bearing signal either through its passive membrane properties or in the process of spike generation. As shown by the present analysis, these changes can also increase signal-to-noise at the output which in turn lessen the demand for extreme modifications of synaptic input. In other words, high frequency phase comparison is a complex process which is likely to involve a number of specializations of neural function acting in concert. While this poses a problem for the modeler since the number of possible configurations increases exponentially with the number of

free parameters, in the evolutionary sense every parameter *is* more or less free. In this perspective, it is probably more reasonable to expect that the system as a whole will be optimized both because repeated mutations affecting a single parameter are unlikely and because some parameters cannot be modified alone without disrupting some important functional balance. For sound localization, in addition to mechanisms which improve the synaptic input signal or the detection capabilities of the laminaris neuron, further processing e.g. by lateral inhibition can contribute to the overall performance of the system. Because these mechanisms operate in series, the dramatic improvements in frequency response culminating in the barn owl's ability to localize high frequency signals may be due to numerous, but less dramatic changes in neural mechanism at several steps along the "time" pathway (references).

As discussed previously, the pattern of synaptic input is dependent on the shape and duration of each synaptic conductance change. This in turn depends on the time course of neurotransmitter-receptor binding and of subsequent channel gating. That is, although transmitter release is triggered by action potentials in the pre-synaptic terminal, the time course of the post-synaptic conductance change is not directly linked to that of the pre-synaptic voltage change. There are several intermediate sites at which decreases in synaptic duration can be effected where speed limitations posed by membrane capacitance are not relevant. First, it is well established that transmitter release is controlled by the presence of  $Ca^{++}$  in the pre-synaptic terminal. Therefore, if  $Ca^{++}$  is prevented from lingering in the pre-synaptic terminal by rapid sequestering or binding, or by rapid inactivation of voltage-dependent  $Ca^{++}$  channels, transmitter release can be truncated. As well, the duration of synaptic conductance change can be controlled post-synaptically since chemical synapses generally contain mechanisms by which neurotransmitter is inactivated either by enzymatic degradation or by re-uptake. The post-synaptic receptor-channel itself may also provide a site whereby rapid truncation of conductance could occur. In addition to these molecular mechanisms, structural specializations in the pre-synaptic terminal which restrict transmitter release to a sub-set of pre-positioned vesicles could contribute both to rapid onset and brief duration. Thus, there are a number

of sites whereby the critical parameter of post-synaptic conductance timing could be modified independently of the timing of the pre-synaptic action potential. However, there is evidence both from single unit records of auditory nerve fibers (Sullivan and Konishi 1984) and from neurophonic recordings in laminais (Sullivan and Konishi 1986) that these spikes may themselves be a bit faster than normal.

Although the hypotheses suggested above would indicate that short synaptic durations may be feasible, it is not clear what the lower limits of these processes acting either alone or in series may be. In addition, input simulations suggest that extremely short synaptic durations of 100  $\mu$ sec or less while desirable, may not be necessary if the time course of the post-synaptic conductance change is asymmetrical. The relaxation of assumptions about input timing can also be compensated by modifications of spike output which enable steady and/or low frequency inputs (which are the necessary biproducts of longer synaptic duration) to be filtered out. With longer synaptic durations (i.e. above 1 millisecond or so) the mechanisms proposed herein become less effective as the low frequency noise first equals then surpasses the size of the information bearing signal and as the amount of synaptic modulation relative to background level decreases. Nevertheless, there is obviously some intermediate range in which conservative changes in several parameters can enable clear discrimination of phase differences in high frequency signals.

In models displaying the most robust discrimination, several changes in synaptic and active conductances were made. In general, increases in the density and/or rate of voltage sensitive sodium channels lead to greater sensitivity to all frequencies but this results in reduced selectivity for high frequency modulations at threshold. Unilateral increases in potassium channel density and/or rate first selectively eliminate responses to low frequency and steady inputs but eventually render all inputs ineffective. Increases in all four of these parameters thus enable improved high frequency sensitivity to be combined with high frequency selectivity. The finding that multiple changes in model parameters seem to be required for optimal performance, while reducing the magnitude required of any single change, also raises the question of how these

changes could have co-evolved especially if these parameters are independently regulated genetically. Membrane conductance is a function of individual channel conductance and of channel density. Variations in the former would probably require mutations in each of the genes coding for the channel proteins whereas changes in the latter could be accomplished by gene duplications or by changes in gene regulation. In this respect, the co-regulation of voltage sensitive and synaptic channel density could be accomplished at the regulatory level. Furthermore, this arrangement would be adaptive since it allows appropriate impedance balances to be maintained. Similarly, increases in gating rate of the voltage sensitive channels can be individually controlled at the level of the channel genes or globally by factors such as temperature. Global changes in gating rate was found to be a more efficient way of increasing high frequency selectivity so that a factor of 2 to 3 over the normal rate constants for homeothermic systems may be sufficient. This represents a temperature difference of only ?? degrees Centigrade.

Experimental results suggest that laminaris neurons in the 5 kHz range have maximum modulations of about 50%. Although the present analysis shows that this is not the theoretical upper limit, further processing in the time pathway can augment this initial ITD filtering, rendering further improvements in laminaris unnecessary. Recent work by Fujita and Konishi shows that ITD tuning may be sharpened by GABAergic lateral inhibition ---

Testability of the model -